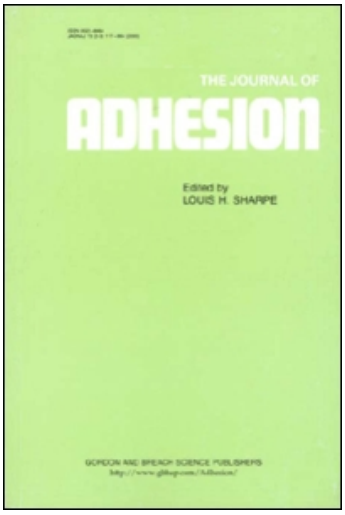

The Journal of Adhesion

Publication details, including instructions for authors and subscription information:
http://www.informaworld.com/smpp/title~content=t713453635

Study of Adherence of Elastomers by Cyclic Unloading Experiments

M. Barquins[a]; D. Wehbi[b]
[a] Laboratoire Central des Ponts et Chaussees, Equipe de Recherche de MScanique des Surfaces du C. N. R. S., Paris, FRANCE [b] Laboratoire de Microanalyse des Surfaces, Ecole Nationale Supérieure de Mécanique et des Microtechniques, Besançon, FRANCE

To cite this Article Barquins, M. and Wehbi, D.(1986) 'Study of Adherence of Elastomers by Cyclic Unloading Experiments', The Journal of Adhesion, 20: 1, 55 — 74
To link to this Article: DOI: 10.1080/00218468608073239
URL: http://dx.doi.org/10.1080/00218468608073239

J. Adhesion, 1986, Vol. 20, pp. 55–74
0021-8464/86/2001–0055 $18.50/0

Printed in the United Kingdom

Study of Adherence of Elastomers by Cyclic Unloading Experiments

M. BARQUINS

Equipe de Recherche de Mécanique des Surfaces du C.N.R.S., Laboratoire Central des Ponts et Chaussées, Paris, FRANCE.

D. WEHBI

Laboratoire de Microanalyse des Surfaces, Ecole Nationale Supérieure de Mécanique et des Microtechniques, Besançon, FRANCE

(Received October 25, 1985; in final form February 1, 1986)

We have studied the time evolution of the contact area between a spherical punch and a half-space elastomer sample by means of a cyclic push-on/pull-off test. The contact area edge is assumed to be a crack tip which propagates in the interface, moving backward and forward. It is shown that the equation of the kinetics of adherence, proposed in 1978 by Maugis and Barquins[3] $G - w = w\phi(a_T \cdot v)$, linking the strain energy release rate G, the Dupré energy of adhesion w and the function ϕ characteristic of the viscoelastic material tested, is valid if w takes two particular values. The first, w_1, depends on the initial contact time, the second, $w_2 < w_1$, depends on the compression time. These values are calculated theoretically according to Johnson *et al.*[2] by measuring the contact area radius. Thanks to this kinetic law, we can predict the number of cycles needed for separating the materials in contact. Moreover, it stresses the fact that the rupture does not occur if the application time of the tensile force is below a certain critical value. The experimental data obtained with a spherical glass punch on the flat surface of a polyurethane sample reproduce the theoretical predictions faithfully.

KEY WORDS Adherence; Crack propagation; Cyclic loading; Elastomers; Fracture mechanics; Polyurethane.

INTRODUCTION

In 1881, Hertz[1] established the theory of the contact between a rigid sphere and an elastic half-space. However, as it was pointed out by

Johnson *et al.*[2] in 1971, Hertz's calculations do not take into account the attractive molecular forces (Van der Waals's forces in the case of elastomers) which contribute to the increase of the contact area and of the punch penetration into the elastic material.

The approach taken by Johnson *et al.*[2] was based on the study of the energy balance, the contact area under a given load being that which minimizes the total energy (elastic, potential and surface energy). Therefore, even for a zero load, the contact area has a finite value and a breaking strain is required for separating the two surfaces. Maugis and Barquins[3] have shown that this theory is an application of Griffith's theory[4] to brittle fracture since the contact rupture does not occur suddenly but progressively and can be considered as a crack propagating inwards along the interface. Therefore, the equilibrium state of two solids brought into contact corresponds to the case $G = w$ where

G = strain energy release rate
$w = \gamma_1 + \gamma_2 - \gamma_{12}$ = Dupré's energy of adhesion
γ_1 = surface energy of the punch
γ_2 = surface energy of the sample
γ_{12} = surface energy of the interface punch-sample.

For a given contact area A, the equilibrium is stable for $\partial G/\partial A > 0$; it is unstable for $\partial G/\partial A < 0$, the elastic force of adherence being the force corresponding to the particular case $\partial G/\partial A = 0$. The equilibrium can be disrupted if the applied load or the elastic displacement are modified (in this case, G is no longer equal to w). For $G > w$, the contact area decreases as the crack moves forward (opening mode I). Inversely, for $G < w$, the contact area increases as the crack moves backward (healing). The difference $G - w$ represents the crack extension force applied to the crack tip. It is the motive force of the crack. Under this force, the crack takes a limiting speed v which depends on the temperature.

Assuming that the viscoelastic losses are proportional to w, as was suggested by Gent and Schultz[5] in 1972, and that they are localized at the crack tip, thus implying that gross displacements remain wholly elastic, we can write[3]

$$G - w = w\phi(a_T \cdot v) \tag{1}$$

The second member represents the viscous drag due to the losses

at the crack tip and $\phi(a_T \cdot v)$ is a dimensionless function depending on the crack speed v and on the temperature through the shift factor a_T of the Williams, Landel and Ferry[6] (WLF) transformation. ϕ is characteristic of the viscoelastic material and is directly linked to the frequency dependence of the imaginary component of the Young's modulus.[7]

The interest of Eq. (1) is that surface properties (w) and viscoelastic losses (ϕ) are clearly decoupled from the elastic properties, the system geometry and the loading conditions, which only appear in G. Experiments carried out with a spherical or a flat punch in contact with elastomer surfaces under fixed load,[3] fixed grips[8] and fixed crosshead velocity[9] as well as peeling experiments[3,5,10,11] have shown that ϕ varies within a wide range of propagation speeds, as

$$\phi = \alpha(T)v^n \tag{2}$$

where $\alpha(T)$ and n are parameters which depend respectively on the temperature and on the tested material. Thanks to the empirical function ϕ we can predict the rupture kinetics in every case. Such a prediction presupposes that rupture is adhesive and the application of Eq. (1) implies that gross displacements are purely elastic. Maugis and Barquins[12] have shown that the speed of the crack propagation is greater when the applied load is increased than when it is decreased. This phenomenon arises from the fact that the strain energy release rate, which is directly linked to the stress intensity factor, cannot be negative and that, for $G = 0$, an increase in the contact area (closing crack) is due to an instantaneous elastic loading characterized by a vanishing crack profile (tangential junction) until the contact area calculated by Hertz is reached. Then, the crack is moved backward very slowly by the motive force $w - G$.

Consequently, when pull-off experiments under fixed loads are performed the rupture time is all the longer (*e.g.*, the elastomers are all the more adhesive) as the contact time is long (dwell-time effect). There has been a twofold interpretation of the increase of adherence with respect to the initial contact time: the former is due to the macroscopic creep of the elastomer which both undergoes deformation and "wets" the surface of the punch,[13] and the latter to the microscopic diffusion of the free ends of the polymeric chains across the interface.[14]

As regards the glass-elastomer contact, Barquins[15] showed that the increase of adherence was caused by the release of the elastic energy that was stored in the asperities particularly compressed in the contact area. This additional energy is never taken into account in the determination of the energy release rate G. Thus, an increase in the initial contact time brings about the decrease of the crack motive force $G - w$ and slows down the separation process through the decrease of G. The $G - w$ decrease can also be interpreted as an increase in the apparent Dupré's energy w. This assumption has the advantage to give a very simple representation of the contact area evolution when the spherical punch is submitted to push-on/pull-off tests.

Our aim is to show that the cyclic loading test allows an experimental selection of two apparent values of $w : w_1$ for a long contact dwell time, $w_2 < w_1$ for a shorter time. Moreover, we will show that we can predict the time evolution of the contact area and of the punch penetration along with the number of cycles needed for observing the complete contact rupture.

ADHESIVE CONTACT

In 1965, Sneddon[16] generalized Hertz's calculations to surfaces of any shape having axial symmetry by using Hankel's transform and Abel's integral. It was shown[17] that the proposed solution allowed for the study of adhesive contacts if an integration constant was supposed to be non-zero. This constant is proportional to the stress intensity factor at the contact area edge, so that the calculation of the normal stress and the discontinuity of the displacement lead to formulae identical to those of fracture mechanics in mode *I* (opening mode). Therefore, the contact area edge can be seen as a crack tip which propagates in the interface, moving backward and forward as the applied load increases or decreases.

The edge of the contact area, like any three-dimensional crack, is subjected locally to a plane strain state,[18] so that the strain energy release rate G is linked to the stress intensity factor K_I by

$$G = \frac{1}{2} \cdot \frac{1 - \nu^2}{E} \cdot K_I^2$$

where E and ν are the Young's modulus and the Poisson ratio respectively ($\nu \simeq 0.5$ for elastomers). The factor 1/2 accounts for the punch rigidity. In the case of a rigid sphere of radius R, the stress intensity factor can be expressed with respect to the applied load P and the contact radius a[17]

$$K_I = \frac{\frac{a^3 K}{R} - P}{(4\pi a^3)^{1/2}}$$

where

$$K = \frac{4E}{3(1-\nu^2)}$$

Thus, the strain energy release rate G connected with the radius a of the contact area can be written

$$G = \frac{\left(\frac{a^3 K}{R} - P\right)^2}{6\pi a^3 K} \tag{3}$$

as well as the elastic displacement d

$$d = \frac{a^2}{3R} + \frac{2P}{3aK} \tag{4}$$

In the equilibrium state, $G = w$ so that Eq. (3) and (4) allow the calculation of the equilibrium values of a and d

$$a = \left\{\frac{PR}{K}\left[1 + \frac{3\pi wR}{P} + \left(\frac{6\pi wR}{P} + \left(\frac{3\pi wR}{P}\right)^2\right)^{1/2}\right]\right\}^{1/3} \tag{5}$$

$$d = \frac{a^2}{R} - \left(\frac{8\pi wa}{3K}\right)^{1/2} \tag{6}$$

Equation (5) proves to be similar to that of Johnson *et al.*[2] based on the study of the energy balance.

Sneddon's[16] equations applied to an adhesive contact[17] reveal that the junction of the elastic solid to the sphere is vertical (fracture mechanics geometry) as is shown in Figure 1. For comparison we have also represented the tangent junction which is given by Hertz's theory for the same applied load. Both kinds of junction can be

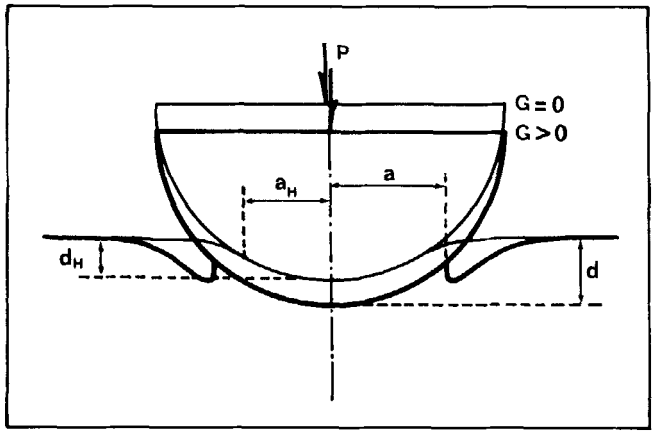

FIGURE 1 Geometry of adhesive contact in equilibrium for a rigid sphere on an elastic half-space. For comparison, Hertzian contact under the same load is also given (fine line).

easily recognized by using an interferometric technique.[12] Thus, the term in brackets in Eq. (5) brings in a corrective factor to Hertz's theory which must be taken into account when the applied load is weak. For instance, under a zero load the contact radius has a finite value

$$a_{P=0} = \left(\frac{6\pi w R^2}{K}\right)^{1/3}$$

Under a slightly negative load a stable contact area can be observed as well. The limit load corresponding to the stability is $P_c = -\frac{3}{2}\pi w R$ which satisfies

$$\left(\frac{6\pi w R}{P} + \left(\frac{3\pi w R}{P}\right)^2\right)^{1/2} = 0$$

in Eq. (5). Under this specific load, the crack propagates instantaneously leading to a complete separation. The value of P_c is independent of the mechanical properties of the material. It represents the elastic adherence force of a spherical punch in contact with an elastic half-space in a fixed load test.

Figure 2 illustrates the equilibrium relations for an adhesive contact (curve $G = w$) and for a non adhesive Hertzian contact

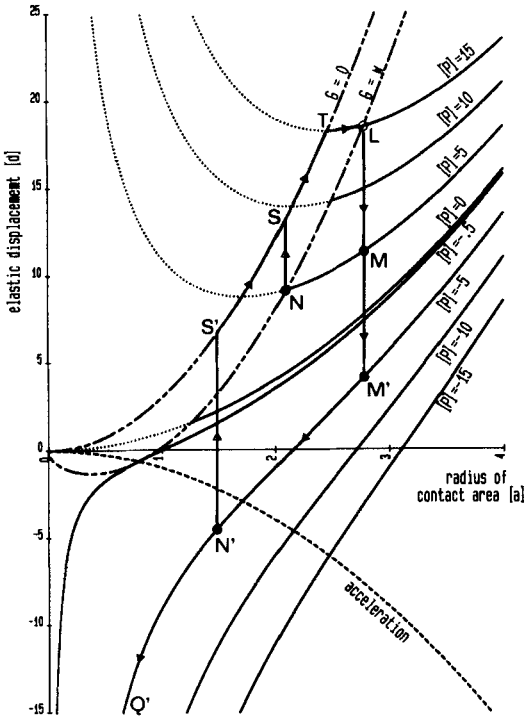

FIGURE 2 The elastic displacement d variations according to the contact area radius a, in reduced coordinates. $G = w$ represents the equilibrium curve; curves $[P]$ show the variation of d with respect to a at fixed load P. Curve $G = 0$ is given by Hertz's theory.

(curve $G = 0$) in reduced coordinates

$$[d] = \frac{d}{\left(\frac{\pi^2 w^2 R}{3K^2}\right)^{1/3}}; \qquad [a] = \frac{a}{\left(\frac{3\pi w R^2}{K}\right)^{1/3}}$$

The variations of the elastic dispalcement with the contact radius are also recorded under well defined loads $\left(\text{curves } [P] \text{ where } [P] = \frac{P}{3\pi w R}\right)$. These curves are independent of the Dupré adhesion energy. Their minima, when they exist (for $P > 0$), are all localized

on Hertz's curve[3] ($G = 0$). If starting from the equilibrium state under a P_0 load (Figure 2 point L), the punch is submitted to a $P < P_0$ load, the equilibrium is upset and the strain energy release rate G reaches an instantaneous value greater than w, whereas the contact area decreases.

Similar experiments[3] performed with a spherical glass punch on a polyurethane sample have shown that d decreases instantaneously whereas a remains constant, thus illustrating the elastic response of the system (part LM or LM' on Figure 2). This variation is followed by a simultaneous variation of a and d under the fixed load P along the corresponding curve $[P]$. Consequently if $P > P_c$ a new equilibrium state can be observed (part MN). Inversely if $P < P_c$ fracture occurs (part $M'Q'$). The propagation kinetics along curve $[P]$ can be studied by means of Eq. (1), G being calculated from Eq. (3). Moreover, it has been shown[3] that the crack speed decreases or increases according to whether $(\partial G/\partial a)p$ is positive or negative. The boundary between the two behaviors is plotted on a dotted curve (Figure 2).

Starting either from point N corresponding to an equilibrium state or from point N' corresponding to an unloading under a force P, the punch is submitted again to the P_0 load. Then, a continuous evolution takes place in two successive phases.[12] The first (part NT or $N'T$ on Figure 2) is instantaneous and corresponds to the elastic response of the sample. It starts with a displacement variation, the radius a remaining constant (part NS or $N'S'$) and G varying from w to 0.

From $G = 0$, the evolution follows the branch ST or $S'T$ according to Hertz's theory. In this first phase, the stress intensity factor is equal to zero and the junction of the half-space to the punch is tangent.

The second phase (branch TL) illustrates the closing of the crack under a constant P_0 load. In this case, G varies from 0 to w and the junction is vertical. It is then possible, as is shown in Figure 2, to carry out a cyclic push-on/pull-off test between two fixed loads P_0 and P, which on the one hand involves the existence of two instantaneous phases (LM' and $N'T$) and on the other hand two phases characterized by a slow kinetics ($M'N'$ and TL).

For the evolution along the branches LM' or $N'T$ the energy dissipation is quasi null. For the evolution along the branches $M'N'$

or TL the viscoelastic losses are located at the crack tip. Furthermore, the contact dwell time effect under the load P_0 can be observed. In other words, using Eqs. (1) and (2), the cyclic push-on/pull-off test allows knowledge of the continuous variation of the contact radius until the separation occurs.

EXPERIMENTAL

The experimental set up (Figure 3), which was used for studying the elastomer adherence under fixed load,[3] consists essentially of a precision balance supporting at the end of one arm a hemispherical glass lens of radius R. This indenter is applied for a duration t under a compressive load P, against the flat surface of an elastomer. A tensile force P' is applied to the end of the other arm by means of an electro-magnet for a duration t'. The contact area, illuminated by reflection of monochromatic light, is observed through the lens with a microscope. For a quantitative evaluation of the contact area evolution, a 16-mm camera records the contact areas at 50 frames/s with approximately tenfold magnification; the contact radii are then measured on the enlarged frames. Besides, an inductive transducer allows the displacements d of the indenter in the sample to be measured continuously.

The tested material is a polyurethane (PSM4 Vishay, $E = 5.4\,\text{MPa}$, $\nu \simeq 0.5$) sample, recommended for dynamic studies in photoelasticity, showing an optically smooth surface.

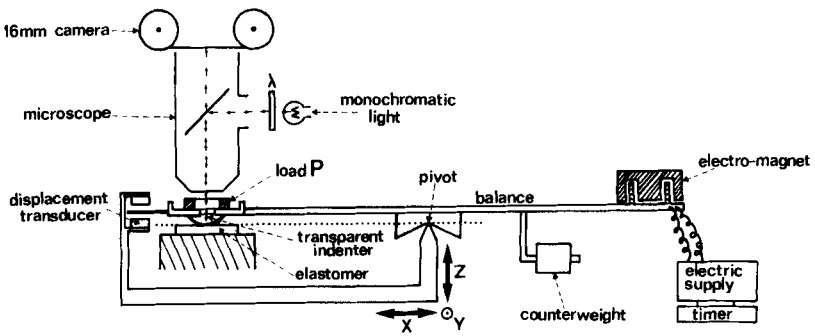

FIGURE 3 Schematic arrangement of the apparatus used to study the adherence kinetics of elastomeric materials under cyclic loading.

Previous experiments about the peeling of this material in contact with a glass surface[3] or with the same material,[19] the unloading of spherical or flat glass indenters under fixed load,[3,15] fixed grips[8] or fixed crosshead velocity,[9] have shown that the dissipation function ϕ characterizing this material varies as $v^{0.6}$ within a wide speed range (10^{-1}–10^{4} μm/s). Moreover, when it is brought into contact with glass, this material shows an adhesion energy w of 30 to 100 mJ/m^2 according to the ambient humidity[11,20] and to the initial compression time.[15]

The sample surface as well as the lens surface were cleaned before each test with alcohol, dried in warm air and left for 30 min until the equilibrium with room atmosphere was reached. The samples failed to exhibit any surface feature such as exuding substances or dust which would have altered the adhesion energy value during the tests.[21]

RESULTS AND DISCUSSION

Figure 4 illustrates the time evolution of the contact radius for a cyclic unloading ($P' = -30$ mN, $t' = 5$ s) and loading ($P = 30$ mN, $t = 1$ s) test (curve I). Curve II shows comparatively the time evolution of the contact radius for a continuous unloading ($P' = -30$ mN), the other parameters being the same as in curve I: indenter radius = 2.19 mm, initial compressive load $P = 30$ mN, initial contact time to = 10 min, temperature = 23°C, humidity = 41%. As it is predictable, according to the fact that the experimental conditions are similar, both curves are superimposed in the first stage of unloading. In curve I, the separation occurred after 11 loading cycles, *i.e.*, after 71 s. In curve II, it occurred 26 s earlier, *i.e.*, after only 45 s. It was predictable that the cyclic loading test which is similar to a fatigue test under fixed load, would delay the separation. However, the loading duration 11×1 s = 11 s does not account for the 26 s delay. Thus, the actual 15 s delay is due to the particular separation kinetics which takes place in such a cyclic test. When an unloading stage is followed by a loading stage, the contact area exhibits two different zones: the first, in the central position, is circular and corresponds to a contact time longer or equal to the initial time t_0; the second corresponding to the peripheral area, is

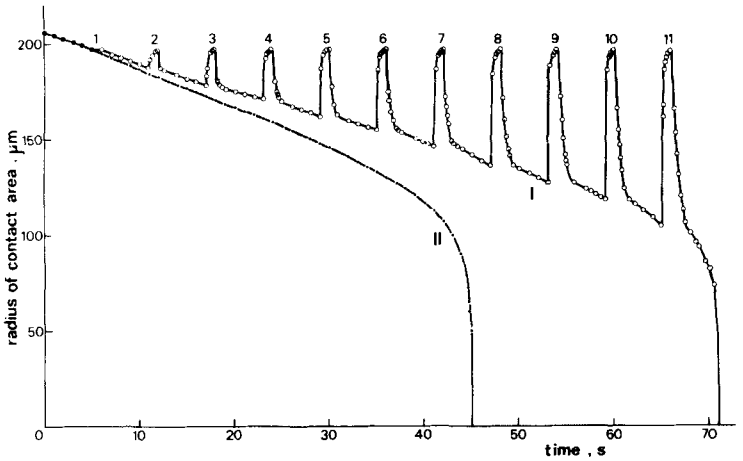

FIGURE 4 Curve I: time evolution of the contact radius of a spherical glass punch on a polyurethane surface submitted to a cyclic loading. Punch radius $R = 2.19$ mm; Compressive load $P = 30$ mN; loading time $t = 1$ s; tensile load $P' = -30$ mN; unloading time $t' = 5$ s. Curve II: time evolution of the contact radius when the surface is submitted to a continuous unloading $P' = -30$ mN.

annular and periodically brought into contact with the indenter for approximately $t' = 1$ s. Though it is a short time, it allows the partial healing of the contact when the crack recedes in the annular area. As a result, the following unloading effect does not occur instantaneously in this area, as is shown in curve I, Figure 4. Therefore, the kinetics of the crack propagation in opening mode in the peripheral zone causes the separation to be delayed in the cyclic loading test.

For an initial contact time $t_0 = 10$ min, the initial contact radius is $a_0 = 206.5\ \mu$m and the corresponding adhesion energy, calculated by using Eq. (5), is $w_1 = 46.4$ mJ/m^2. Under the same conditions, the Hertz contact radius would be $a_H = 190\ \mu$m ($w = 0$). As is shown in Figure 4, after each loading cycle the contact radius is greater than $a_H : a = 197\ \mu$m. Consequently, the contact is adhesive and the corresponding adhesion energy calculated by using Eq. (5) is $w_2 = 9$ mJ/m^2. Thus, we can consider that the central and the peripheral zones of the contact area are characterized by $w_1 = 46.4$ mJ/m^2 and $w_2 = 9$ mJ/m^2 respectively.

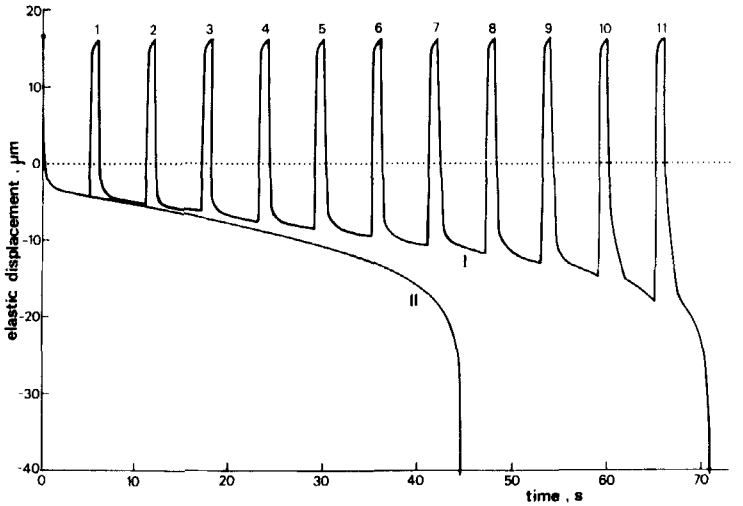

FIGURE 5 Time evolution of the elastic displacement of the punch under the same conditions as in Figure 4. Curve I: cyclic loading, Curve II: continuous unloading.

Figure 5 represents the time evolution of the displacement d measured during the previous cyclic (curve I) and continuous (curve II) unloadings. d values are positive when the lowest point of the indenter is below the level of the sample surface, they are negative when it is above.

Figure 6 shows the d variations according to a. The data are deduced from Figures 4 and 5, the obtained diagram is similar to that of Figure 2. We can notice that the slow kinetic phases correspond to the curves $P' = -30$ mN and $P = 30$ mN, and that the quasi instantaneous propagations occur either for a constant contact radius or along Hertz's curve ($G = 0$). This fact points out that the tested material has purely elastic gross displacements.

For each value of a, it is now possible to calculate the strain energy release rate G (Eq. (3)) and the associated crack speed $v = da/dt$. The $G(v)$ variations corresponding to the crack propagation in a zone which always remains in contact with the punch, are illustrated on Figure 7 (lower dotted line). The values obtained for the cyclic or for the continuous unloadings are quasi identical.

Using Eq. (1) and considering $w = w_1 = 46.4$ mJ/m^2 (central zone) we have also recorded the dissipation function variations $\phi(a_T \cdot v)$

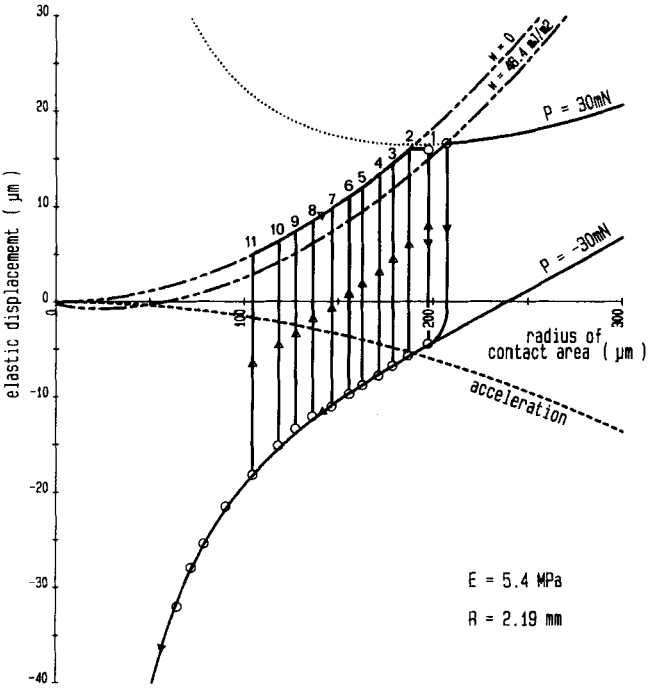

FIGURE 6 The elastic displacement variations according to the contact radius for a cyclic loading from $P = 30$ mN to $P' = -30$ mN. The data are deduced from Figures 4 and 5.

according to v (upper line). On this log–log scale, ϕ appears to vary as $v^{0.6}$ which bears out the previous results.[3,9,15] It is then possible to perform a graphic determination, from Figure 7, of the coefficients $\alpha(T)$ which is only dependent on temperature in Eq. (2). $\alpha(T) = 1.68 \times 10^5$ SI units.

Taking a different approach and assuming that the dissipation function is well defined for this specific material,

$$\phi = 1.68 \times 10^5 \cdot v^{0.6}$$

we can simulate the time evolution of a (Eq. (5)) and d (Eq. (6)) by means of a numerical integration of the general Eq. (1). G is calculated by using Eq. (3) for $P = -30$ mN; a is obtained by using Eq. (5) for $w = w_1 = 46.4$ mJ/m^2 when the crack propagates in the central zone and $w = w_2 = 9$ mJ/m^2 when it propagates in the

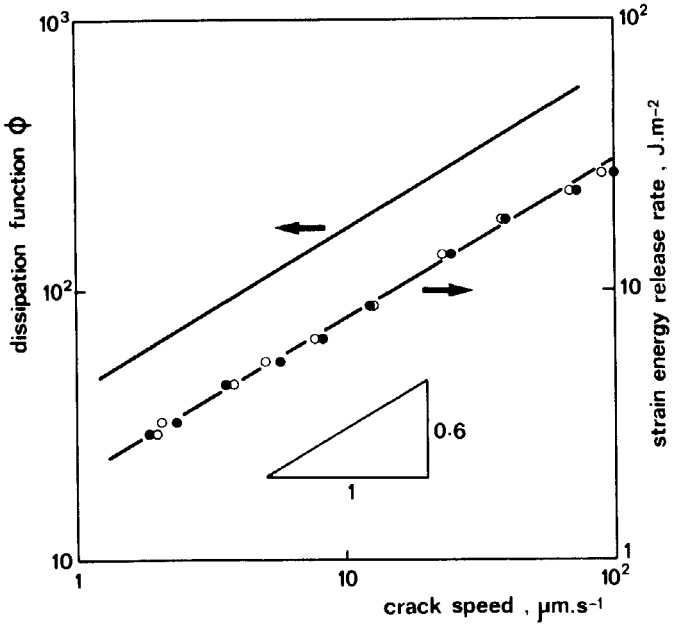

FIGURE 7 The strain energy release rate G and the dissipation function ϕ variations according to the crack propagation speed v, shown on a log–log scale. $G(v)$ is shown by the broken line (cyclic (○) and continuous (●) unloading), the full line represents $\phi(v)$ which varies as the 0.6th power of v.

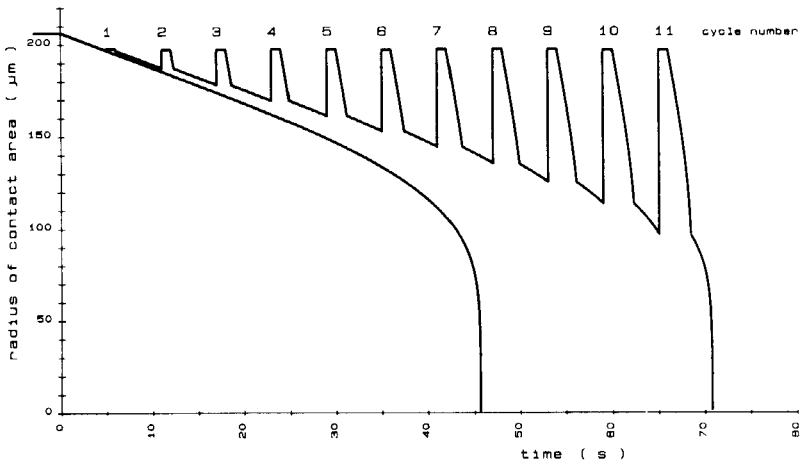

FIGURE 8 Computed curves corresponding to Figure 4.

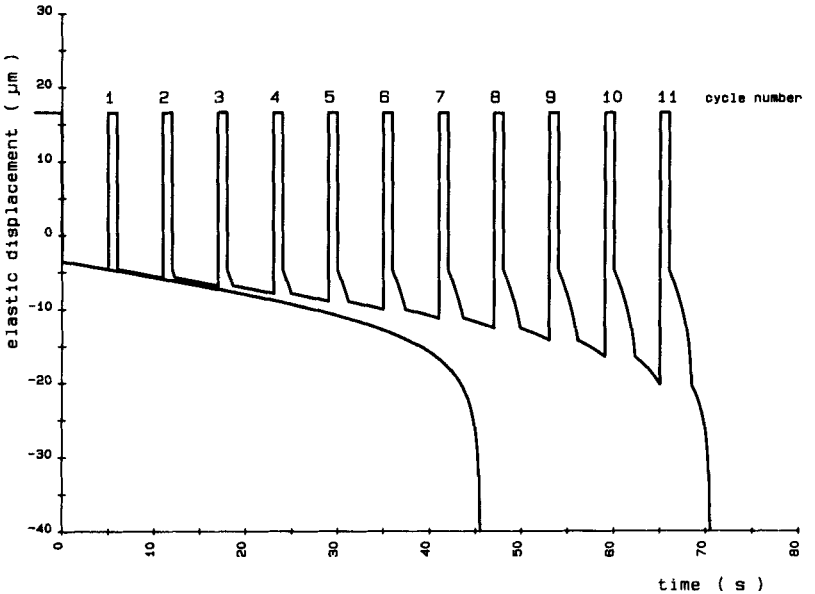

FIGURE 9 Computed curves corresponding to Figure 5.

peripheral zone. The simulated curves are presented in Figures 8 and 9. It is reasonable to assume $w = w_1$ in the central zone since the experiment lasts a short time (71 s) compared to the initial contact time (10 min). In the second case, curve I Figure 4 shows that the contact time which is equal to 1 s for the first cycles reaches 2.5 s for the last ones. Thus w_2 only represents a mean value of the actual adhesion energies characterizing each point of the peripheral zone (the higher values being those on the central zone boundary). Nevertheless, the simulated (Figures 8 and 9) and the experimental (Figures 4 and 5) curves are quite similar. This is also noticeable when the experimental (Figure 6) and the simulated (Figure 10) variations of d according to a, are compared. Thus, the validity of the kinetic model proposed for describing a cyclic loading test is confirmed.

Thanks to this simulation, it is possible to predict the number of cycles needed for observing the complete contact rupture in any circumstance. For example, Table I shows comparatively the experimental and the theoretical numbers of cycles for different

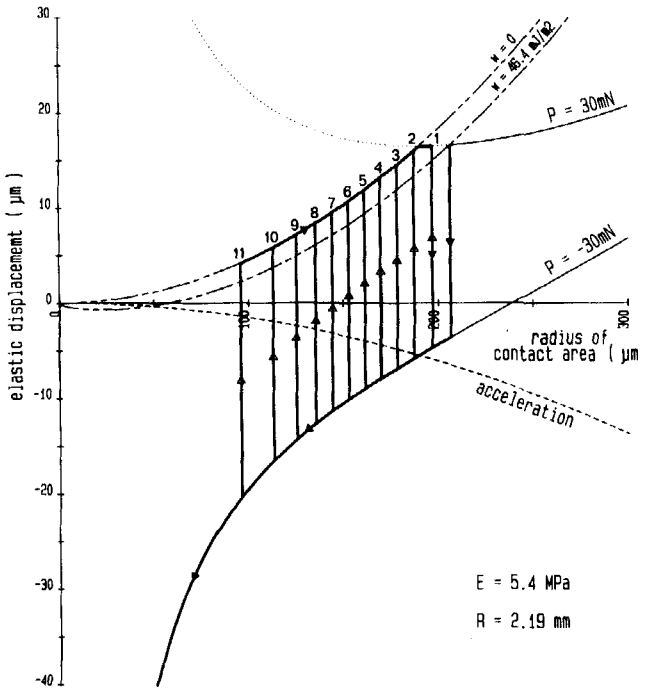

FIGURE 10 The elastic displacement variations with respect to the contact radius for a cyclic loading from $P = 30$ mN to $P' = -30$ mN. The data are deduced from the computed curves shown in Figures 4 and 5 (Figure 10 is to be compared to Figure 6).

TABLE I
Influence of the loading amplitude on the number of cycles leading to the contact rupture ($t = 1$ s, $t' = 5$ s)

Loading P (mN)	Unloading P' (mN)	Number of cycles	
		computed	measured
50	−50	4	4
40	−40	6	6
30	−30	11	11
20	−20	36	40

TABLE II
Influence of the unloading time on the number of cycles leading to the contact rupture ($P = 30$ mN, $P' = -30$ mN, $t = 1$ s)

Unloading time t' (s)	Number of cycles	
	computed	measured
10	5	5
6	9	9
5	11	11
4	16	16
3	30	32
2	∞	$>10^4$

applied loads. As was expected, a decrease in the applied loads delays the separation. However, we should bear in mind that increasing the number of cycles leads to an increase in the contact time in the central zone which in turn increases adherence.[15] This is the reason why, beyond a certain value, the simulated numbers of cycles become less than the experimental ones.

We have also studied the role of the unloading time for a fixed loading time (Table II). We notice that a decrease in the unloading time increases the number of cycles needed for observing the separation. If the delay is not too long, the contact dwell time effect remains negligible and the proposed kinetic model applies; *i.e.*, the number of cycles which are predicted is equal to the number of cycles which are actually observed.

Moreover, under our experimental conditions, it was shown that for an unloading time less than 3 s, contact rupture did not occur. In this case, a stable cycle took place, the contact radius varying between two fixed values 130 and 197 μm for $t' = 2$ s as is shown in Figure 11. This phenomenon is directly linked to the propagation kinetics of the contact area edge in the peripheral zone. The width of this zone which increases during the first cycles, rapidly becomes wide enough so that, during t', the crack propagates without penetrating in the central zone.

A stable propagation cycle can also take place when the loading time is particularly increased. In this case, the adhesion energy w_2 characterizing the peripheral zone increases, slowing down the crack propagation during the next unloadings.

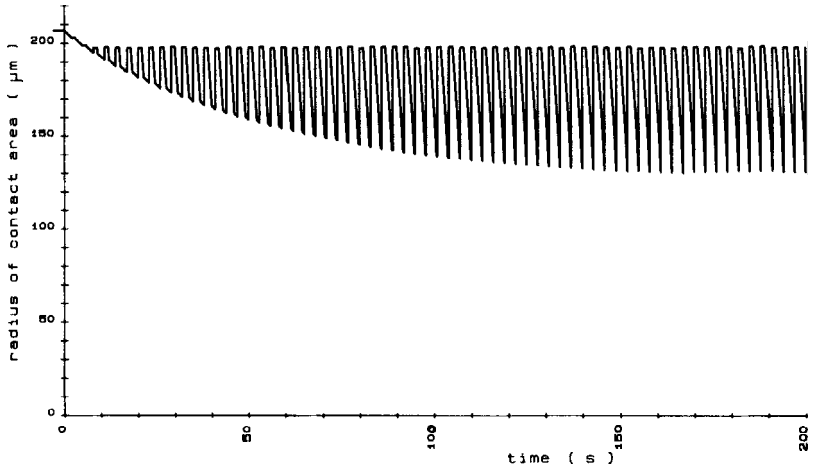

FIGURE 11 Computed curve representing the time evolution of the contact radius for cyclic unloadings of short duration ($P = 30$ mN, $t = 1$ s; $P' = -30$ mN, $t' = 2$ s). A stable cycle takes place and the contact rupture will not be observed.

CONCLUSIONS

Fracture mechanics concepts can be applied to the study of the adherence kinetics of a rigid spherical indenter in contact with the flat surface of a half-space elastomer sample submitted to a cyclic loading test. The general equation used in previous studies about the unloading of spherical or flat glass indenters under fixed load,[3,15] fixed grips[8] or fixed crosshead velocity[9]

$$G - w = w\phi(a_T \cdot v)$$

has been successfully applied to the study of the adherence of elastomers by cyclic unloading experiments.

The knowledge of the dissipation function ϕ, which only depends on the temperature through the WLF transformation factor a_T and on the crack speed, allows the prediction of the adherence kinetics in any case provided that gross displacements are purely elastic and that the viscoelastic losses are localized at the crack tip. Within a wide speed range, ϕ can be described by

$$\phi(a_T \cdot v) = \alpha(T)v^n$$

where $n = 0.6$ for polyurethane.[3,19] Assuming two values of w calculated using Johnson *et al.*'s theory,[2] the first w_1 specific to long contact times, the second $w_2 < w_1$ specific to shorter contact times, Eq. (1) allows the following predictions

1) Rupture is not observed in a cyclic loading test under certain conditions if it failed to be observed in a continuous unloading test under similar conditions.

2) Cyclic unloading tests compared to continuous unloading tests delay the contact rupture. The delay is due to the partial healing of the contact during the loading phases.

3) The occurrence of the complete rupture depends on the unloading time.

4) For short unloading times, a stable cycle takes place so that one might think that the fatigue of an adhesive contact cannot be observed for a purely viscoelastic material, *i.e.*, if the crack tip is left undamaged.

The experimental results obtained for a spherical indenter in contact with the flat surface of a half-space polyurethane sample (PSM4 Vishay) reproduce the theoretical predictions faithfully.

Acknowledgements

The authors are indebted to the DRET and to the GRECO 46 for the financial support of this work.

References

1. H. Hertz, *J. für die Reine und Angewandte Mathematik* **92,** 156 (1881).
2. K. L. Johnson, K. Kendall and A. D. Roberts, *Proc. Roy. Soc. Lond. A* **324,** 301 (1971).
3. D. Maugis and M. Barquins, *J. Phys. D: Appl. Phys.* **11,** 1989 (1978).
4. A. A. Griffith, *Phil. Trans.* **A221,** 163 (1920).
5. A. N. Gent and J. Schultz, *J. Adhesion* **3,** 281 (1972).
6. M. L. Williams, R. F. Landel and J. D. Ferry, *J. Amer. Chem. Soc.* **77,** 3701 (1955).
7. G. Ramond, M. Pastor, D. Maugis and M. Barquins, *Rev. G.F.R.* in press.
8. M. Barquins, *J. Appl. Polym. Sci.* **28,** 2647 (1983).
9. M. Barquins and D. Maugis, *J. Adhesion* **13,** 53 (1981).
10. K. Kendall, *J. Phys. D: Appl. Phys.* **6,** 1782 (1973).
11. A. D. Roberts, *Rubber Chem. Tech.* **52,** 23 (1979).

12. D. Maugis and M. Barquins, in *Adhesion and Adsorption of Polymers* 12A, L. H. Lee, Ed. (Plenum Press, New York, 1980), p. 203–277.
13. R. Bates, *J. Appl. Polym. Sci.* **20,** 2941 (1976).
14. G. Koszterszitz, *Colloid and Polymer Sci.* **258,** 685 (1980).
15. M. Barquins, *J. Adhesion* **14,** 63 (1982).
16. I. N. Sneddon, *Int. J. Engng. Sci.* **3,** 47 (1965).
17. M. Barquins and D. Maugis, *J.M.T.A.* **1,** 331 (1982).
18. M. K. Kassir and G. C. Sih, *J. Appl. Mech.* **33,** 601 (1966).
19. M. Barquins, *J. Appl. Polym. Sci.* **29,** 3269 (1984).
20. M. Barquins, *Etude théorique et expérimentale de la cinétique de l'adhérence des élastomères,* Theseis, Paris, (1980).
21. A. D. Roberts and A. B. Othman, *Wear* **42,** 119 (1977).